FAILURE ANALYSIS OF COMPOSITE PRESSURE VESSELS BASED ON THE ENHANCED FILAMENT WINDING SIMULATION: COMPARING LAYER-BASED AND FIBER BUNDLE-BASED APPROACHES

Jörg B. Multhoff[1]

[1]ISATEC GmbH, Rathausstr. 10, 52074 Aachen, Germany
Email: j.multhoff@isatec-aachen.de, Web Page: http://www.isatec-aachen.de

Keywords: Fiber Bundle Model, Composite Pressure Vessel, Structural Analysis

Abstract
Filament-wound composite pressure vessels are usually modeled using a multi-layered approach based on the classical laminate theory. Given the realities of practical filament-wound vessels, this approach may not be satisfactory in critical areas like the polar openings and turning zones, with respect to transition patterns or when faced with layers lacking full surface coverage. Effects of band stacking or effects due to the finite band-width may not be represented sufficiently by the layered approach, as the relevant model data (fiber angle and layer thickness) is not uniquely defined. A new approach motivated by the tenets of netting analysis and based on a finite element formulation with an embedded fiber-bundle model is being explored. This approach can be seen as an extension of modeling with reinforcing elements and is implemented as a generalization of layered finite element formulations. The necessary model input data in the form of the fiber-bundle trajectories is generated using an enhanced filament winding simulation. Results of this new approach are compared with models based on classical layered finite elements. This work leads to an improved understanding of the stress state in production filament-wound composite pressure vessels and thus enables more accurate design by analysis procedures. Furthermore, the improved modeling of discontinuous and non-layered fiber architectures may enable optimizations relying on the combined use of filament winding, over-braiding and fiber placement for the construction of composite pressure vessels.

1. Introduction

The interest in gas storage for mobile applications is steadily growing. This leads to a rising demand for light-weight composite pressure vessels. However, the behavior of composite structures is unintuitive and not easy to predict. The safe and efficient design of composite pressure vessels therefore requires thorough analysis. Filament winding is one of the oldest manufacturing methods for structural composites [1]. Wet winding has the advantages of using the raw materials, fiber and resin, in its direct form without intermediate processing steps. The manufacturing speed measured in mass per time is among the highest in comparison to other methods. In sum, this contributes to relatively low manufacturing costs for filament wound composite materials compared to other methods and explains its continued importance. In the filament winding process multiple rowings or tows, each composed of thousands of fibers, are formed to a flat band and are impregnated with a matrix material, usually a resin. The band is continuously deposited on a rotating mandrel, eventually covering the entire surface. The resulting winding pattern consists of multiple cycles, in each cycle the band follows a specific path along the winding surface, Fig. 1. This path is characterized by a certain angle α of the band and thus the fibers relative to

Excerpt from ISBN 978-3-00-053387-7

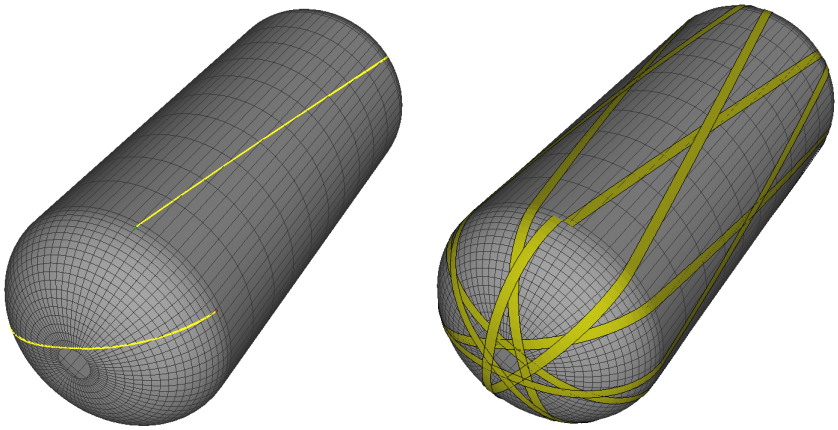

Figure 1. Fiber path (left) and unidirectional band (right) on the winding surface [2].

the *meridian* of the winding surface. Usually the cylindrical part of the vessel is covered in such a way that the resulting layer is composed of two bands with opposing fiber angles ($+\alpha/-\alpha$) at each location.

2. Filament Winding Simulation

The effects of the filament winding process on the resulting fiber architecture is not self-evident and requires analysis by filament winding simulation.

2.1. Fiber Path

The wet fiber can be deposited on the surface only on – or close to – a geodesic path without slipping. On a surface of revolution with local radius r the geodesic path is given by Clairaut's theorem [1**?**]: $r\sin(\alpha) = \text{const}$. The fiber is tangent at the polar opening with radius r_p, i.e. $\alpha(r_p) = 90°$. These layers are called helical layers. For geodetic winding the fiber angle at each radius can be evaluated by Eqn. (1). Fig. 2.2 shows an example for this fiber angle distribution. Some deviation from this path is possible if the surface friction or material adhesion is exploited.

$$\alpha(r) = \arcsin\left(\frac{r_p}{r}\right) \tag{1}$$

Layers with a constant winding angle close to 90° are called hoop layers and can only be applied in the cylindrical part of the vessel. The polar opening radius of these layers is equal to or close to the radius in the cylindrical part of the vessel. Practical designs require multiple helical and hoop layers each with different winding angle α_0 and corresponding polar opening diameters.

2.2. Layer Thickness

One feature of the continuos filament winding process is that each *parallel* of the winding surface is crossed by the same number of fibers. This results in a constant layer thickness in the cylindrical part of the vessel. However, the layer thickness increases with decreasing vessel radius. This is a consequence of the progressive band overlap that can be easily recognized in Fig. 1 and Fig. 3. The resulting layer thickness distribution is shown in Fig. 2.2. This behavior can be approximately described by Eqn. (2) up to a certain distance from the polar opening.

Excerpt from ISBN 978-3-00-053387-7

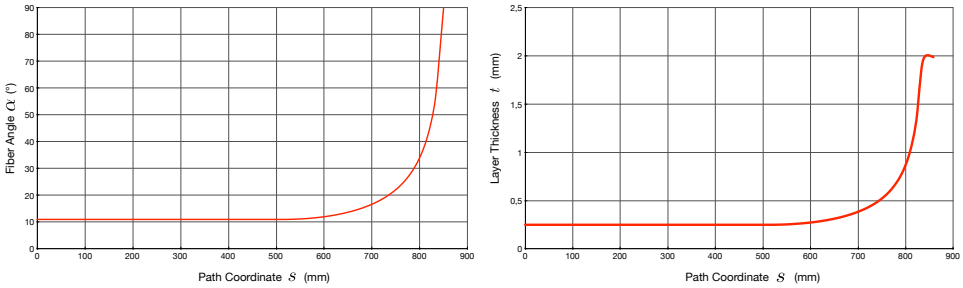

Figure 2. Example for fiber angle (left) and thickness distribution (right).

$$t(r) = t_0 \frac{r_0 \cos(\alpha_0)}{r \cos(\alpha)} \tag{2}$$

Improved prediction of the layer thickness is possible by empirical or analytical methods and by the enhanced filament winding simulation.

2.3. Enhanced Filament Winding Simulation

The main differences between the real fiber architecture of filament wound vessels and the idealized theory as described above can be recognized by explicit consideration of the finite fiber band width w in an enhanced version of the filament winding simulation. After computing the fiber path, the geometry of the fiber band, usually consisting of multiple parallel fiber strands, is modeled, Fig 1. The fiber band is represented by patches of triangles connecting consecutive bounding points. The local thickness is computed by accumulation of band patches at sampling points on the winding surface. Likewise the local laminate stacking sequence at any sampling point can be computed. Details are presented in [2].

2.4. Local Laminate Properties

The main results of the simulated band deposition on the winding surface are consistent with observations that can also be made with actual vessels manufactured by filament winding. The differences between the real laminate structure and the idealized theory are mainly due to the finite width w of the filament band. They are reduced with decreasing width of the band. Additional differences may exist due to fiber bridging effects. The main observations are:

1. The effective thickness distribution along the meridian direction is not continuos as shown in Fig. 2.2. But stepped due to the band overlap.
2. The thickness at a given meridian position in circumferential direction is not constant but variable and depends on the winding pattern.
3. The local fiber angle within a layer at a given meridian and circumferential position is not constant in the circumferential direction (Fig. 3) and is in general not given by Clairaut's theorem as shown in Fig. 2.2

In sum the important local properties fiber angle and layer thickness possess a discontinuous distribution in the laminate. For optimized composite pressure vessel designs it is of high interest to examine the effects of these observations on the structural behavior.

Excerpt from ISBN 978-3-00-053387-7

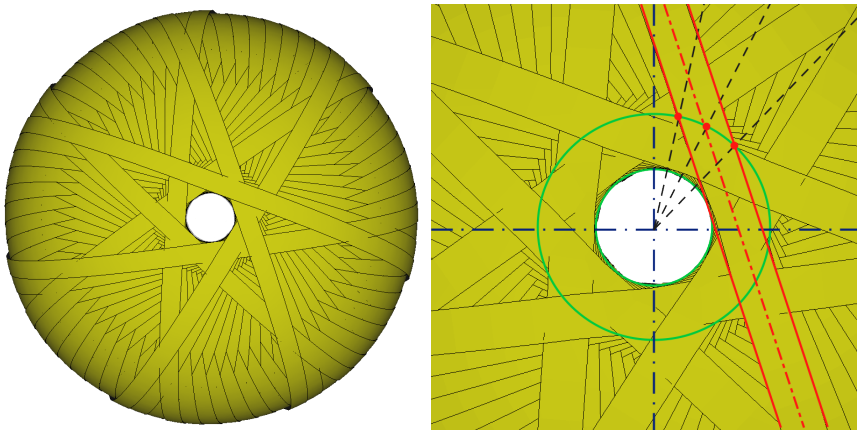

Figure 3. Overlap of the unidirectional band in the dome (left) and especially near the polar opening (right) [2].

2.5. Representation of Local Properties in the Analysis Model

The transfer of the laminate data generated by the enhanced filament winding simulation into the finite element model may proceed as follows: In the simplest case, the grid points representing the winding surface are used as nodal points of the finite element discretization. The finite elements may be shell or solid elements. However, only solid elements allow for the required detailed analysis. In the case of solid elements the grid points represent the nodes on the inner surface and the nodes on the outside surface are generated using the normal vectors of the winding surface and the thickness data. The required thickness information for each node is taken from the accumulated band thickness at the nodal points. Depending on the element type, the internal laminate description may allow for multiple layers with constant thickness and constant angle of principle material direction or for variable thickness layers with variable angle of principle material direction. In the latter case, the thickness and angle data usually have to be input at the nodal points. However, most finite element formulations require that the layers are continuous within the element and thus that the number of layers is the same at all nodes.

It turns out that this may not be the case for general filament wound structures. The easiest solution to this problem is to use a sampling point in the center of the element to record the local laminate stacking sequence and to use this data to define the laminate corresponding to the entire element. This may represent the real stiffness and strength distribution poorly. A more accurate approach may be to use the location of the in-plane integration points of the element as the sampling points, e.g. for 4 x 4 in-plane Gauss integration. Different laminate stacking sequences with individual number of layers would result at the in-plane integration points, making special element formulations necessary. A mesh layout which respects the detailed description of the real laminate as shown e.g. in Fig. 3 within the framework of a laminate theory is hard to envision.

To avoid the mentioned problems, in the present research the filament wound band is modeled as a group of fiber bundles following the real fiber path on the winding surface. The fiber bundles are embedded in a structured mesh representing the matrix material.

3. Finite Element Analysis of Composite Pressure Vessels

The finite element analysis of composite laminates based on the assumptions of the classical laminate theory is described e.g. in [3]. The most appropriate representation, especially for thick-walled vessels, can be achieved using layered solid elements. In general multiple elements in thickness direction are

Excerpt from ISBN 978-3-00-053387-7

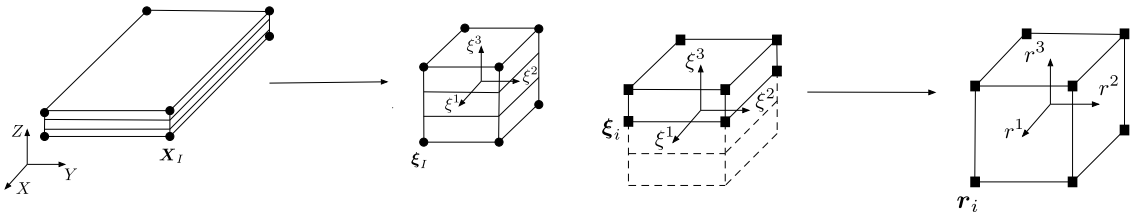

Figure 4. First and second isoparametric map for integration of layered elements [4].

necessary.

3.1. Layered Solid Element

An element formulation allowing for variable element thickness – among other features – is proposed in [4]. Here only the integration scheme for the linear stiffness matrix is considered. The element geometry is interpolated with tri-linear shape functions. After the first isoparametric map a second isoparametric map for each layer is introduced, Fig. 4. The coordinates $\boldsymbol{\xi} = [\xi^1, \xi^2, \xi^3]^T$ of the first map are interpolated in terms of the coordinates $\boldsymbol{r} = [r^1, r^2, r^3]^T$ of the second map using Eqn. (3) and (4). $\boldsymbol{\xi_i}$ contains the coordinates of the layer under consideration.

$$\boldsymbol{\xi} = \sum_{i=1}^{nnode} \bar{N}_i \boldsymbol{\xi_i} \tag{3}$$

$$\bar{N}_i = \frac{1}{8}(1 + r^1 r_i^1)(1 + r^2 r_i^2)(1 + r^3 r_i^3) \tag{4}$$

The components of the element stiffness matrix $\boldsymbol{K}_{eIJ}$ are evaluated by summation over all layers *nlay* and over all integration points *ngaus*:

$$\boldsymbol{K}_{eIJ} = \sum_{L=1}^{nlay} \sum_{gp=1}^{ngaus} \boldsymbol{B}_I^T(\boldsymbol{\xi}_{gp}^L) \mathbb{C}_L \boldsymbol{B}_J(\boldsymbol{\xi}_{gp}^L) \det \boldsymbol{J}(\boldsymbol{\xi}_{gp}^L) \det \boldsymbol{J}^L(\boldsymbol{r}_{gp}^L) w_{gp}^L \tag{5}$$

Here, $\boldsymbol{J}$ and $\boldsymbol{J}^L$ are the Jacobian matrix of the first and second map and w_{gp}^L are the weighting factors of the integration point. $\boldsymbol{B}$ is the strain interpolation matrix and $\mathbb{C}_L$ is the constitutive matrix in layer L. For the modeling of a filament wound structure with a stack of layered solid elements with variable layer thickness the total laminate must be mapped on the laminate pertaining to the individual elements.

3.2. Reinforcing Element

The application of truss elements embedded in solid elements for the modeling of dry filament wound pressure vessels was proposed in [5]. This can be realized by constraining the nodal degrees of freedom of the truss element to the degrees of freedom of the embedding solid element. Thus the displacement field of the solid element imposes the displacements of all embedded truss elements. The same effect can be achieved by classical reinforcing elements as described e.g. in [6]. Here, the degrees of freedom of the reinforcing element $\{u_{II}, v_{JJ}, w_{II}\}^T$ are expressed in terms of the degrees of freedom of the embedding element $\{u_i, v_i, w_i\}^T$ by way of the eight tri-linear shape functions of the embedding element N_i by Eqn. (6), Fig. 5.

Excerpt from ISBN 978-3-00-053387-7

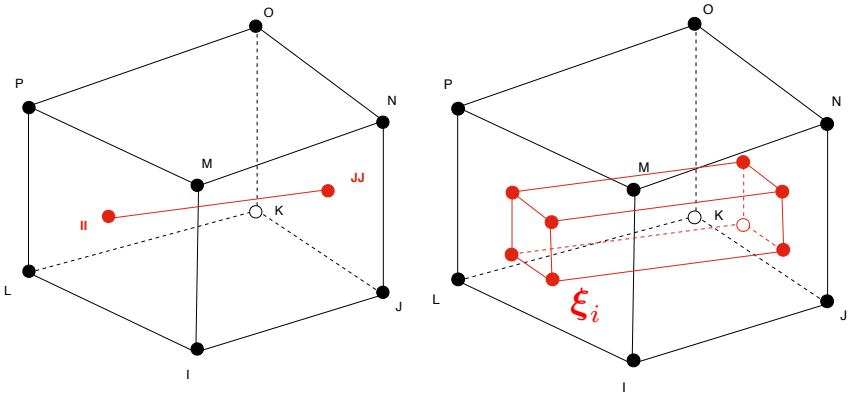

Figure 5. Reinforcing element embedded in a solid element (left). Schematic of the fiber bundle element (right).

$$\begin{Bmatrix} u_{II} \\ v_{II} \\ w_{II} \end{Bmatrix} = \sum_{i=1}^{8} N_i(\xi_{II}, \eta_{II}, \zeta_{II}) \begin{Bmatrix} u_i \\ v_i \\ w_i \end{Bmatrix} \tag{6}$$

Using this transformation the stiffness matrix of the reinforcing element can be expressed in terms of the degrees of freedom of the embedding element and superimposed to form the total stiffness. Typically, the reinforcing element allows the definition of multiple reinforcing members. This formulation is restricted to unidirectional reinforcement in the direction of the reinforcing members. For the modeling of a filament wound structure the global fiber architecture must be mapped on the reinforcing members in the individual elements.

3.3. Fiber Bundle Element

The idea of the fiber bundle element is to form a synthesis of the layered element and the reinforcing element as a practical meso-level model for the fiber architectures arising from filament winding. Each fiber bundle is modeled by a volume simply computed from length and cross section area. This is similar to the reinforcing element described before, but allows the alternative use of a one-dimensional or a three-dimensional constitutive model. In the latter case the reinforcement is not purely unidirectional. The components of the element stiffness matrix are evaluated as follows:

$$\boldsymbol{K}_{eIJ} = \sum_{B=1}^{nbundle} \sum_{ip=1}^{nip} \boldsymbol{B}_I^T(\boldsymbol{\xi}_{ip}^B) \mathbb{C}_B \boldsymbol{B}_J(\boldsymbol{\xi}_{ip}^B) \det \boldsymbol{J}(\boldsymbol{\xi}_{ip}^B) \det \boldsymbol{J}^B(\boldsymbol{r}_{ip}^B) w_{ip}^B \tag{7}$$

The differences between variants are the number of integration points, the effective formulas for the Jacobian matrix of the second isoparametric map $\boldsymbol{J}^B$ and the weighting factor w_{ip}^B of the integration points. $\mathbb{C}_B$ is the constitutive matrix for the fiber bundle B.

4. Results

As a prove of concept an isotensoid shell is analyzed using one model with layered elements and another model using reinforcing elements. The diameter of the shell is 1000 mm, the polar opening diameter is 100 mm and the band with is 24 mm. The composite overwrap is modeled using the enhanced filament winding simulation. The resulting winding pattern, band overlap and thickness distribution are shown in

Excerpt from ISBN 978-3-00-053387-7

Fig. 6. The thickness distribution is not continuous in meridian direction and not uniform in circumferential direction. The model using layered elements is derived by averaging the thickness distribution in circumferential direction. The model using reinforcing elements is generated by mapping the 12 rovings forming the band on the appropriate elements. The results for the two models are compared in Fig. 7. The deformed shape is show for a meridian cross section for a model based on the layered approach and a model using reinforcing elements. The stress distribution for both models is given in Fig. 8. The continuous line show the layer stress in fiber direction on the top and bottom of the shell for the model based on the layered element. The dots show the stress in fiber direction for the individual segments at each meridian position. The model using layered elements represents average effects while the model using reinforcing elements is able to represent considerably more detail.

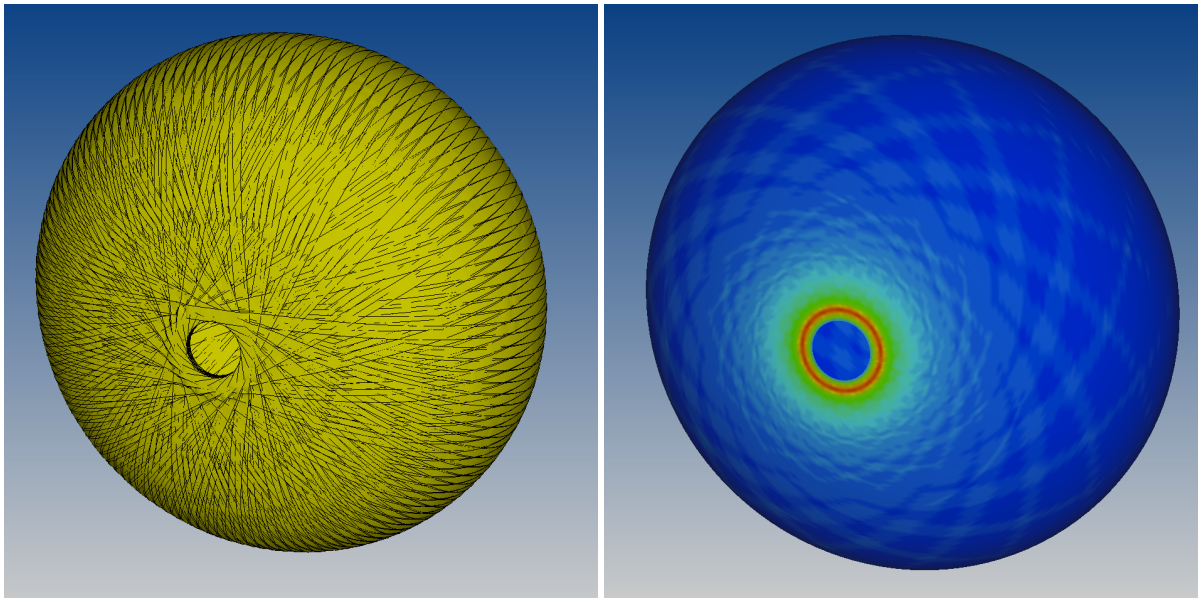

Figure 6. Modeling of the composite shell: Overlapping bands on isotensoid shape (left). Resulting non-uniform thickness distribution (right).

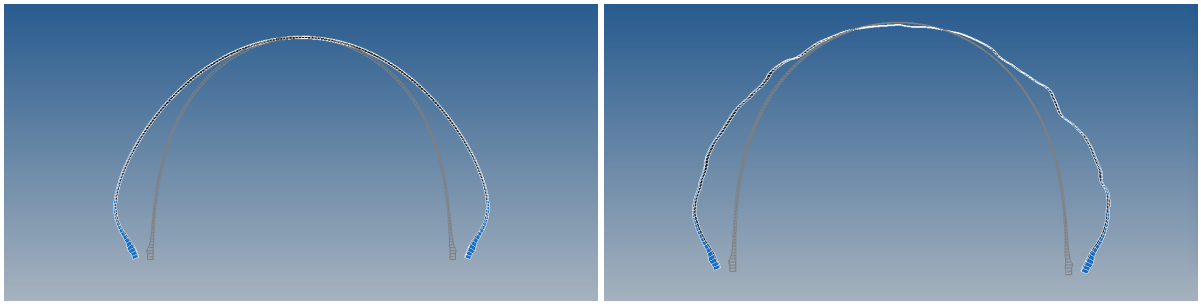

Figure 7. Deformed shape under internal pressure for one meridian cross section (scaled): Axisymmetric idealization using layered elements (left). Computation based on enhanced filament winding simulation using reinforcing elements (right).

5. Conclusion

The present work proves the concept of modeling filament wound pressure vessels using the enhanced filament winding simulation and using reinforcing elements. A more realistic representation of the filament wound structure can be achieved. Further work is necessary for the full implementation of the

Excerpt from ISBN 978-3-00-053387-7

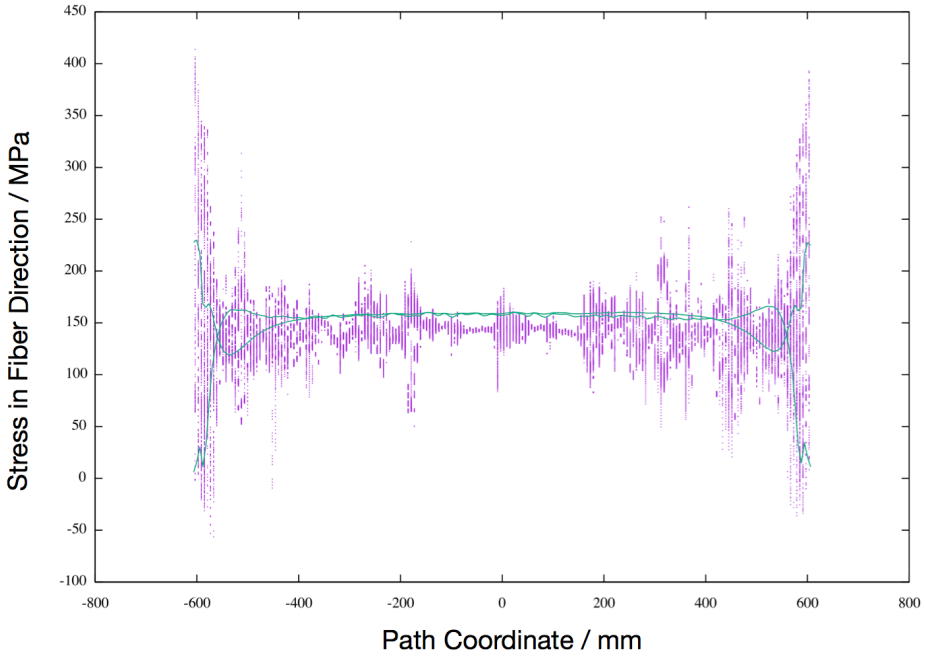

Figure 8. Distribution of the stress in fiber direction for one meridian cross section of the shell: The layered model is represented by the continuous lines, showing the inside and outside of the shell. For each segment in the reinforcing elements a dot is displayed.

fiber bundle element and for a more efficient mapping of the data generated with the filament winding simulation onto the finite element mesh.

References

[1] S.T. Peters, W.D. Humphrey, R.F. Foral, *Filament Winding Composite Structure Fabrication*. 2nd Edition. SAMPE Publishers, 1999.

[2] J.B. Multhoff, Enhanced Filament Winding Simulation for Improved Structural Analysis of Composite Pressure Vessels. *The 19th International Conference on Composite Materials*, Montreal, 2013.

[3] O.O. Ochoa, J.N. Reddy, *Finite Element Analysis of Composite Laminates*. Kluwer Academic Publishers, 1992.

[4] S. Klinkel, F. Gruttmann, W. Wagner, A continuum based three-dimensional shell element for laminated structures. *Computers and Structures*, Vol. **71**, 43–62, 1999.

[5] J.J. Koppert, H. de Boer, A.P.D. Weustink, A. Beukers, H.E.N. Bersee, Virtual Testing of Dry Filament Wound Thick Walled Pressure Vessels. *The 16th International Conference on Composite Materials*, Kyoto, 2007.

[6] G. Hofstetter, H.A. Mang, *Computational Mechanics of Reinforced Concrete Structures*. Vieweg, 1995.

Excerpt from ISBN 978-3-00-053387-7